

# Scientific Herald of Uzhhorod University Series “Physics”

Journal homepage: <https://physics.uz.ua/en>

Issue 49, 54-60

Received: 20.12.2020. Revised: 24.02.2021. Accepted: 26.04.2021



УДК 539.173+539.173.8+5393.1.6

PACS 24.75.+1, 25.85.-w, 25.85.Ec, 25.85. Ca

DOI: 10.24144/2415-8038.2021.49.54-60

## Structure of Mass-Yield Distributions of $^{232}\text{Th}$ Photofission Product by Bremsstrahlung at Energy 17.5 MeV

Oleg O. Parlag, Vladimir T. Maslyuk, Eugene V. Oleynikov, Igor V. Pylypchynets\*,  
Alexander I. Lengyel

Institute of Electron Physics, National Academy of Sciences of Ukraine,  
88017, 21 Universytetska Str., Uzhhorod, Ukraine

### Abstract

**Relevance.** One of the most promising areas for studying the fission process is to investigate its features under the action of photon radiation, since the interaction of gamma quanta with the nucleus is completely electromagnetic with well-known characteristics. Information on the yields of  $^{232}\text{Th}$  nuclear photofission products is of particular interest from the standpoint of experimental and theoretical studies. The nucleus of this element is located on the border between pre-actinides and light actinides.

**Purpose.** The purpose of this study is to experimentally investigate the structure of the mass distribution of yields of  $^{232}\text{Th}$  photofission products at a bremsstrahlung energy of 17.5 MeV (energy close to the threshold of the first-chance fission, where experimental data are not available).

**Methods.**  $^{232}\text{Th}$  photofission response was simulated on the electron accelerator of the Institute of Electron Physics NAS of Ukraine – M-30 microtron. The bremsstrahlung spectrum was modelled for the case of electron interaction ( $E=17.5$  MeV) with a tantalum converter (1 mm) using the GEANT4 code 10.7. Yields of  $^{232}\text{Th}$  photofission products were measured by gamma-ray spectrometry. The yields of  $^{232}\text{Th}$  photofission products were modelled using the GEF 2020 / 1.1 and Talys 1.95 codes.

**Results.** The value of cumulative yields of 23 products ( $^{85\text{m}}\text{Kr}$ ,  $^{88}\text{Kr}$ ,  $^{88}\text{Rb}$ ,  $^{89}\text{Rb}$ ,  $^{91}\text{Sr}$ ,  $^{92}\text{Sr}$ ,  $^{94}\text{Y}$ ,  $^{95}\text{Zr}$ ,  $^{97}\text{Nb}$ ,  $^{99}\text{Mo}$ ,  $^{101}\text{Tc}$ ,  $^{131}\text{I}$ ,  $^{132}\text{Te}$ ,  $^{133}\text{I}$ ,  $^{134}\text{Te}$ ,  $^{135}\text{I}$ ,  $^{138}\text{Cs}$ ,  $^{139}\text{Ba}$ ,  $^{140}\text{Ba}$ ,  $^{141}\text{Ce}$ ,  $^{142}\text{La}$ ,  $^{143}\text{Ce}$ ,  $^{146}\text{Ce}$ ) belonging to 22 isobaric mass chains (light: 85; 88; 89; 91; 92; 94; 95; 97; 99; 101, heavy: 131; 132; 133; 134; 135; 138; 139; 140; 141; 142; 143; 146 fragments) of the  $^{232}\text{Th}$  photofission was measured at a maximum bremsstrahlung energy of 17.5 MeV (average excitation energy  $\sim 11.3$  MeV). The resulting mass distribution of heavy fragments indicates the presence of increased yields of products localized around mass 133-134, 138-139, and 143-144, which is associated with the influence of such a nuclear structure as the proximity of closed nuclear shells and the even-odd effect.

**Conclusions.** The measurement results indicate the presence of a fine structure in the resulting mass distribution of  $^{232}\text{Th}$  photofission product yields, which is manifested in increased yields of products localised in the mass regions 133-134, 138-139, and 143-144. The obtained theoretical output values calculated using the GEF 2020 / 1.1 and Talys 1.95 codes describe in general terms and predict the fine structure of the mass distribution of  $^{232}\text{Th}$  photofission products

**Keywords:** bremsstrahlung, microtron,  $^{232}\text{Th}$ , gamma-ray spectrometry, first-chance fission

### Suggested Citation:

Parlag OO, Maslyuk VT, Oleynikov EV, Pylypchynets IV, Lengyel AI. Structure of mass-yield distributions of  $^{232}\text{Th}$  photofission product by bremsstrahlung at energy 17.5 MeV. *Scientific Herald of Uzhhorod University. Series “Physics”*. 2021;(49):54-60.

\*Corresponding author

## Introduction

One of the promising areas of studying the fission process is the investigation of the distribution of the yields of fission products under the action of photons, since the nature of such interaction is well-known (it is completely electromagnetic) [1], and allows obtaining fission nuclei with low excitation energy immediately after their absorption. The use of bremsstrahlung photons formed on electron accelerators allow conducting studies in the low-energy range (where the features of the influence of nuclear structure and dynamics on nuclear fission are clearly manifested [2]) and obtain experimental data on the dependence of the mass and charge distributions of photofission products on the excitation energy of fission nuclei.

Existing estimated experimental data for a wide range of nuclei [3] indicate the presence of a fine structure in the mass distributions of photofission product yields [4]. The fine structure is manifested in increased yields of heavy fission products (localised around and near masses 133-134, 138-140, and 143-144) and complementary light yields of fission products [4], which is associated with such an influence of the nuclear structure as the effect of proximity to closed nuclear shells and the odd-even effect [2; 4].

Of particular interest in terms of experimental and theoretical studies is information on the yields of products (post-neutron) of the  $^{232}\text{Th}$  nuclear photofission, which is located on the border between pre-actinides ( $_{88}\text{At}$ ,  $_{89}\text{Ra}$ ) and light actinides ( $_{91}\text{Pa}$ ,  $_{92}\text{U}$ ) [5; 6]. In low-energy fission of isotopes from  $^{221}\text{Th}$  to  $^{230}\text{Th}$ , there is a transition from symmetric to asymmetric fission [7], which is associated with the different probability of development of symmetric and asymmetric fission channels and their influence on the development of mass distributions of fission product yields [2].

Another reason for this interest is the widespread application of the photofission reaction of thorium nuclei [8-9]. Information on the yields of thorium isotope fission products under the action of high-energy photons and fast neutrons plays an important role in the development of a new generation of power generating systems, namely: fast neutron reactors (fuel cycle  $^{232}\text{Th} - ^{233}\text{U}$ ), reactors with accelerators (controlled subcritical systems) [8; 9], as well as for the development of non-destructive methods for isotope analysis of fertile (non-fissionable by thermal neutron) nuclear materials [10]. The above-mentioned applications of the Thorium photofission process also require reliable yield information for a wide range of fission products.

Therefore, in terms of obtaining new experimental results and developing new theoretical approaches (models) to describe the of mass distributions of yields of  $^{232}\text{Th}$  nucleus photofission products, as an object of research, is of particular interest.

*The purpose of this study* is an experimental study of the structure of the mass distribution of yields of  $^{232}\text{Th}$  photofission products at the maximum bremsstrahlung energy of 17.5 MeV and comparison with the simulation results using modern GEF and Talys calculation codes.

## Theoretical Overview

Detailed analysis of existing experimental data indicates the presence of a fine structure in the mass distributions of asymmetric yields of  $^{232}\text{Th}$  nuclear photofission products for the region of bremsstrahlung photon energies ( $E_{\gamma\text{max}}$ ) from 6.5 to 80 MeV, which corresponds to the range of excitation energies ( $E^*$ ) from  $\sim 6$  to  $\sim 22.5$  MeV [11], where there are possible probabilities of “multi-chance fission” reactions [12-14], that is, as emission-free ( $^{232}\text{Th}(\gamma, f) ^{232}\text{Th}$  – first-chance, and fission with pre-emission of one and two neutrons ( $^{232}\text{Th}(\gamma, nf) ^{231}\text{Th}^*$  – second-chance [6; 7];  $^{232}\text{Th}(\gamma, 2nf) ^{230}\text{Th}^*$  – third-chance). At high energies (above the threshold of  $(\gamma, f)$  – reactions), competition occurs between fission processes and neutron emission. After neutron evaporation, the excitation energy of the nucleus decreases due to the binding energy and kinetic energy of the released (evaporated) neutron, which affects the final values of product yields and, accordingly, the fine structure of mass distributions [12-14].

To estimate the boundaries of the energy region where emission-free photofission occurs and with preliminary neutron emission, calculations are made of the probability dependence of the relative contribution of individual chances (the first – without preliminary neutron emission, the second – with the emission of one neutron, and the third – with the emission of two neutrons) on the excitation energy for the fission of the  $^{232}\text{Th}^*$  nucleus using the GEF Code [15; 16]. The results of the calculations are presented in Figure 1.

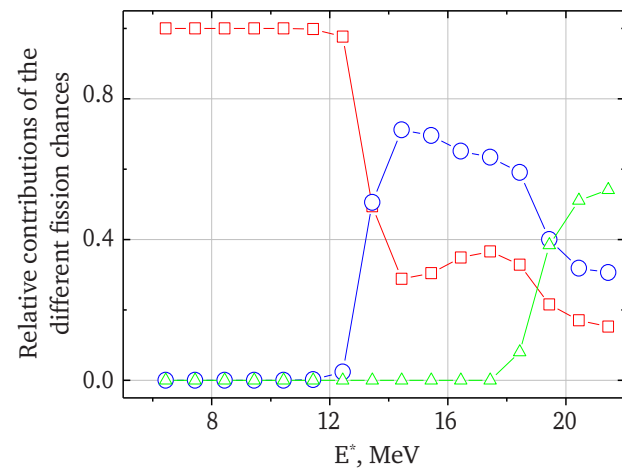


**Figure 1.** Dependence of the relative contribution of individual chance upon  $^{232}\text{Th}^*$  fission from the excitation energy

**Source:** the data obtained by the authors of this study (squares – 1<sup>st</sup>; circles – 2<sup>nd</sup>; triangles – 3<sup>rd</sup>-chance fission)

It is established that the threshold of  $(\gamma, nf)$ -reaction upon  $^{232}\text{Th}$  photofission exceeds  $\sim 11.5$  MeV, which is consistent with the results of modelling the contribution of the reaction cross-sections along the  $(\gamma, f)$  and  $(\gamma, nf)$  channels to the total reaction cross-section of  $(\gamma, F)$  photofission of the  $^{232}\text{Th}$  nucleus as a function of the excitation energy  $E^*$ , conducted in [17; 18] by the Talys calculation code [19] (Fig. 2).

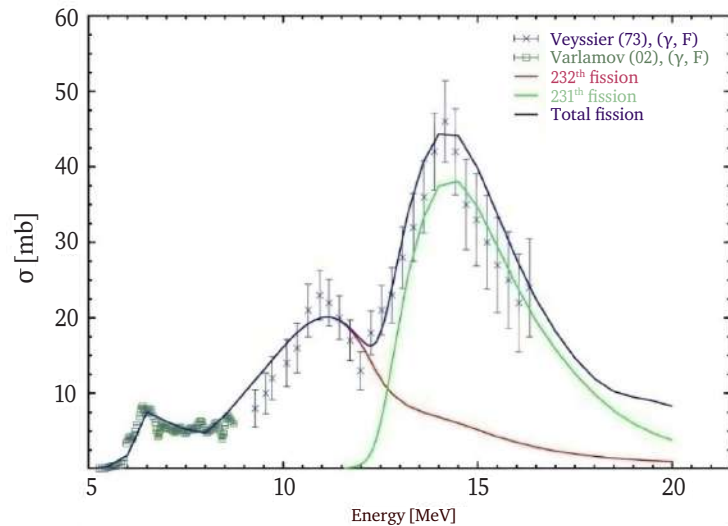


**Figure 2.** Dependence of the reaction cross-section on the excitation energy upon  $^{232}\text{Th}$  nuclear photofission: circles and crosses – experiment,  $(\gamma, F)$  – blue,  $(\gamma, f)$  – red,  $(\gamma, nf)$  – green curves

Source: [17]

Notably, upon fission with an excitation energy  $E^* > 11.5$  MeV, a “mixture of fission nuclei” is developed, the components of which are present in all yields of fission products. Existing (or modern) experimental methods do not allow separating the yields of products from simultaneously developed fissile nuclei without and with preliminary neutron emission. Therefore, it is important to investigate the energy region near the first-chance fission threshold, where experimental data are not available ( $E^* > 11.2$  ( $E_{y_{\max}} = 16$ ) [11] and  $E^* < 12.4$  ( $E_{y_{\max}} = 20$ ) MeV [20]). Existing experimental data set [21] on product yields for a fission core  $^{232}\text{Th}$  at  $E^* \sim 11.28$  MeV ( $E_{y_{\max}} = 17.5$  MeV) describes only the shape of the mass distribution curve of the yields, but does not allow drawing a conclusion about its structure due to the limited number of fission products studied.

## Materials and Methods

Determination of relative cumulative yields of  $^{232}\text{Th}$  photofission products was performed by semiconductor gamma-ray spectrometry [22; 23]. The studied value during measurements is the counting rate in peaks of total absorption (or peak intensity) of gamma quanta from individual fission products, which depends on its activity, absolute measurement efficiency, self-absorption corrections, and gamma line intensity.

### Stimulation of the $^{232}\text{Th}$ photofission reaction

When conducting experimental studies,  $^{232}\text{Th}$  metal foil was used (in the amount of 5 samples, diameter – 12 mm, thickness – 2 microns), the mass of which was in the range of 209 ÷ 281 micrograms. The targets were manufactured at the V.G. Khlopin Radium Institute (Saint Petersburg, Russia) in 1981. To accumulate photofission products during activation, 0.1 mm thick aluminum foil collectors were used, which were installed close to the  $^{232}\text{Th}$  fission targets. Irradiation of a fissile assembly (which consisted of  $^{232}\text{Th}$  disks and collector layers) were performed on an electron accelerator of the Institute of Electron Physics of

the National Academy of Sciences of Ukraine – an M-30 microtron (electron energy  $E = 17.5$  MeV, average beam current  $\sim 4 \mu\text{A}$ ) [14]. The instability of the electron energy during target irradiation did not exceed 0.04 MeV.

To generate bremsstrahlung, a tantalum converter was used (thickness – 1 mm), located at a distance of 22 mm from the output window (Ta, thickness – 50 microns) of the electron output unit. The fission assembly was installed perpendicular to the beam axis at a distance of 50 mm from the Ta converter. The irradiation time of the fission assembly varied from 30 to 210 minutes. The choice of time parameters (irradiation, cooling, and measurement times) was made considering the half-lives of the studied photofission products and their precursors (the so-called “parent” products) along the isobaric chain.

### Simulation of the fission target activation process

The GEANT410.7 computing code was used to simulate the spectra of bremsstrahlung photons, residual electrons, and photoneutrons (depending on the energy normalised per electron) [24]. The input parameters used in the calculations almost completely reproduced the geometric dimensions (design features) of the electron output unit and the activation schemes of fissile nuclei, which was implemented on an electron accelerator – the M-30 microtron.

The simulation considered the geometric dimensions of the original electron beam: the shape – an ellipse, the dimensions of the semi-axes – 11 mm and 3 mm). Calculations were performed for  $10^9$  ( $10\text{E}9$ ) electrons in the initial beam on two computers with 4- and 12-core Intel(R) Core(TM) processors i7-9750H CPU@2.60GHz and 36 GB and 16 GB RAM.

As a result of the simulation, the total number of photons, residual electrons, and photoneutrons normalised per electron hitting a fission target was calculated: 0,08128 photons (with an energy of 6 MeV, involved in stimulating the photofission reaction – 0,01179); – 0,01602 electrons and  $\sim 10^{-5}$  neutrons. Residual electrons and photoneutrons

that fell on the fission assembly did not affect the results of the experiment.

The calculated spectrum of bremsstrahlung photons is presented in Figure 3, where the  $^{232}\text{Th}(\gamma, f)$  reaction

cross-section is additionally provided [25], which was used to calculate the average excitation energy of a fissionable nucleus [11]. Value of the average excitation energies of a fissionable  $^{232}\text{Th}^*$  nucleus was 11.28 MeV.

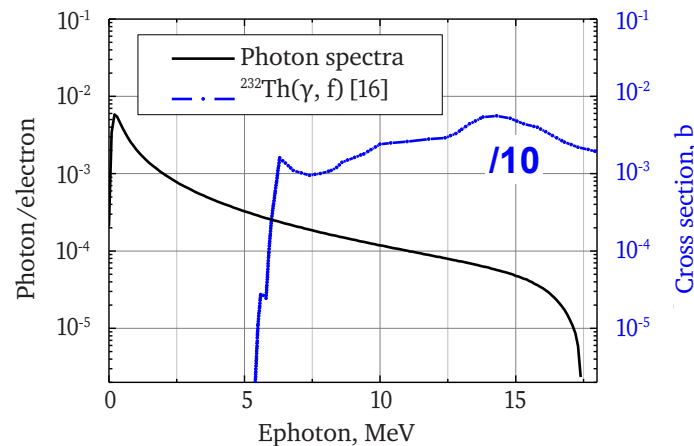


**Figure 3.** Photon spectrum (solid curve) and  $^{232}\text{Th}(\gamma, f)$  reaction cross-section (dashed curve)

Source: [25]

### Gamma-ray spectrometric studies of $^{232}\text{Th}$ photofission products

At the end of the accumulation of fragments, aluminum collectors measured their gamma activity for from 0.25 to 381 hours after the end of irradiation. The duration of individual measurements varied from 0.5 to 6.5 hours. For the research, spectrometric complexes based on semiconductor detectors were used: HPGe (Ortec) and Ge (Li), the volumes of which were 150 and 100 cm<sup>3</sup> with an energy resolution of ~ 2.45 and ~ 3.5 keV for the line  $^{60}\text{Co}$  (1,332.5 keV). When studying the relative cumulative yields of fission products, the final error of the obtained results is primarily affected by the error value of the measured energy efficiency of the detector [13].

The energy dependence of the peak efficiency of gamma-ray quantum registration was determined using a set of standard certified point sources  $^{22}\text{Na}$ ,  $^{57}\text{Co}$ ,  $^{60}\text{Co}$ ,  $^{109}\text{Cd}$ ,  $^{133}\text{Ba}$ ,  $^{137}\text{Cs}$ ,  $^{151}\text{Eu}$ ,  $^{241}\text{Am}$  (produced by D.I. Mendeleev Institute for Metrology, Saint Petersburg, Russia). Additionally, the detectors were calibrated using gamma radiation from the products developed in the  $^{238}\text{U}(\gamma, f)$  reaction stimulated by bremsstrahlung with an energy of 17.5 MeV, and accumulated in aluminum foil [26], which allowed substantially simplifying the measurement process and consider the real geometry. The value of the statistical measurement error during the calibration procedure did not exceed 4%.

Gamma-ray spectra from photofission products were measured in real time. The dead time of the spectrometer did not exceed 8% during all measurements. During the measurements, the drift of the energy scale, resolution and recording efficiency of the spectrometric complex were constantly monitored using point standard gamma-active sources  $^{57}\text{Co}$  and  $^{60}\text{Co}$ . The drift of these parameters did not exceed 1%. Spectroscopic information

was processed using the Winspectrum software package [27]. Fission fragments were identified by the energies of their characteristic gamma lines, considering their half-lives and measurement, accumulation, and cooling times. Additionally, the half-lives of their predecessors along isobaric chains were considered. The values of nuclear spectroscopic data of the identified fission products (energies and intensities of gamma lines, half-lives of the formed products and their precursors along the isobaric chain) were taken for calculations from the NNDC nuclear data library (USA) [28].

### Results and Discussion

During the experiment, the authors measured the peak intensity of gamma lines belonging to the following products of the  $^{232}\text{Th}$  nuclear photofission:  $^{85\text{m}}\text{Kr}$  (151.2),  $^{88}\text{Kr}$  (196.3),  $^{88}\text{Rb}$  (898.03; 1836.0),  $^{89}\text{Rb}$  (1248.1),  $^{91}\text{Sr}$  (1024.3),  $^{92}\text{Sr}$  (1383.9),  $^{94}\text{Y}$  (918.7),  $^{95}\text{Zr}$  (756.7),  $^{97}\text{Nb}$  (658.1),  $^{99}\text{Mo}$  (739.5),  $^{101}\text{Tc}$  (306.8),  $^{131}\text{I}$  (364.5),  $^{132}\text{Te}$  (228.2),  $^{133}\text{I}$  (529.9),  $^{134}\text{Te}$  (767.2),  $^{135}\text{I}$  (1260.4),  $^{138}\text{Cs}$  (1435.8),  $^{139}\text{Ba}$  (165.9),  $^{140}\text{Ba}$  (537.3),  $^{141}\text{Ce}$  (145.4),  $^{142}\text{La}$  (641.3),  $^{143}\text{Ce}$  (293.3),  $^{146}\text{Ce}$  (316.7). The energies of gamma lines are presented in parentheses (in keV).

The statistical error of measurements of the peak intensity of gamma product lines used in the analysis did not exceed 3 ÷ 5% for the entire time interval of measurements. Cumulative yields were determined relative to the yields of the  $^{132}\text{Te}$  reference product.

The total error of relative cumulative yields was estimated considering statistical errors of peak intensity of gamma product lines, analysis of time dependencies, spread of values averaged over individual measurements, as well as errors of interpolated efficiency values and nuclear physical constants (energy and intensity of gamma lines, half-lives of products). The total error in determining the relative cumulative yields of fission fragments did not exceed 8 ÷ 10%.



From the measured relative cumulative yields of fission fragments  $Y_R$  and calculated values  $Z_p$  relative total yields of fission products were determined  $Y_{RT}(A)$ , and summarised on all mass chains [29]:

$$Y_{RT}(A) = \frac{Y_R(C\pi)^{\frac{1}{2}}}{\sum_{Z=1}^{\infty}} \exp\left(-\frac{(Z - Z_p)^2}{C}\right), \quad (1)$$

where  $Y_{RT}(A)$  is the total relative cumulative yields of the mass chain  $A$ ;  $Y_R$  is the relative cumulative yield of a fragment with an atomic charge  $Z$  and a mass number  $A$ ;  $Z_p$  is the most probable charge;  $C$  is the distribution width parameter ( $C=0.6$  [11]).

To calculate the most probable charges  $Z_p$  for individual chains of isobar nuclei, the study used the values of the dependence of the yield of prompt neutrons on the mass  $A$  of light and heavy fragments  $\nu_{L,H}$  and average values of the total neutron yield  $\nu_{tot}$  calculated using semi-empirical formulas [30] and using GEF [16] and Talys 1.95 codes [19].

The obtained value  $\nu_{tot}(\text{parameter})=2.54$  [30], corresponds to the value  $\nu_{tot}(\text{ENDF})=2.41$  from the base of estimated nuclear data ENDF [25] within error of  $\sim 5\%$ , and with values of  $\nu_{tot}(\text{GEF})=2.75$  [16] and  $\nu_{tot}(\text{Talys})=3.03$  [19] within of error  $< 10\%$  and  $< 20\%$ , respectively. The calculated dependences of neutron yields on the mass of light and heavy fragments  $\nu_{L,H}$  upon  $^{232}\text{Th}$  photofission were used to find  $Z_p$ . Relative total yields  $Y_{RT}(A)$  of the resulting fission products summed over all mass chains, normalised to a

total yield of 200% to calculate the absolute yields of mass chains  $Y(A)$ .

Experimental values of total yields of light and heavy  $^{232}\text{Th}$  photofission products at a maximum bremsstrahlung photon energy of 17.5 MeV are represented in Figure 4 by dark squares (light – a, heavy – b). Circles represent yields of fission products at an energy of 16 MeV [11], triangles – yields of fission products at an energy of 20 MeV [20]. The presented experimental data are consistent with each other within the experimental errors for the energy region  $E_{\gamma\text{max}}$  from 16 to 20 MeV (near the threshold of the first-chance fission). At the same time, the measured values of the yields of fission products in this paper and in [21] within experimental errors are consistent with each other. Figure 4 also presents the yields of fission products for a  $^{232}\text{Th}^*$  fission nucleus at an excitation energy of  $\sim 11.28$  MeV, calculated by the GEF code [16] (solid curve and Talys 1.95 code [19] (dashed line), which describe the dependences of product yields on the mass of fragments in general terms and predict their structure. In the resulting mass distribution of yields of  $^{232}\text{Th}$  photofission products, a certain structure is observed (for heavy fragments, the yield of fission products around mass numbers 133-134, 138-139, and 143-145 is increased), which is associated with the influence of asymmetric fission channels on the development of mass distributions, which, in turn, depend on the nuclear structure (the effect of proximity of closed nuclear shells and the odd-even effect) [2; 4; 11; 15].

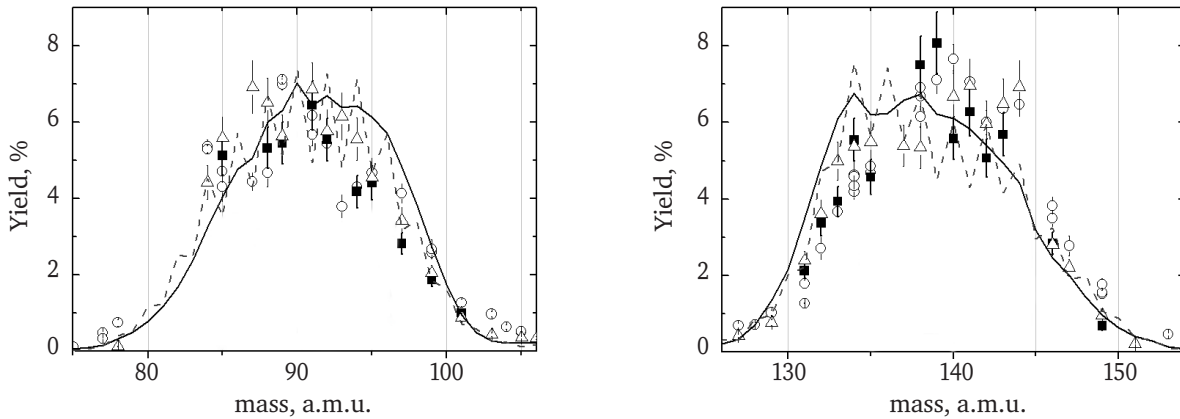


**Figure 4.** Yields of  $^{232}\text{Th}$  photofission products

**Source:** dark squares – data obtained by the authors of this study, circles, triangles, solid curve – GEF 2020/1.1, dotted line – Talys 1.95

## Conclusions

The cumulative yields of 23  $^{232}\text{Th}$  photofission products were determined by semiconductor gamma spectroscopy at the maximum bremsstrahlung photon energy of 17.5 MeV ( $E^* \sim 11.3$  MeV). Full yields of mass chains (light products:  $a = 85; 88; 89; 91; 92; 94; 95; 97; 99; 101$ , heavy products:  $a = 131; 132; 133; 134; 135; 138; 139; 140; 141; 142; 143; 146$ ) were obtained from the aggregate cumulative yields of fission products using corrections for the charge distribution of fragments.

The results obtained and the analysis of existing experimental data indicate a stable presence of a fine structure of the mass distributions of  $^{232}\text{Th}$  photofission products localised for heavy fragments in the vicinity of masses 133-134, 138-139, and 143-145, for the energy region near the threshold of the first-chance fission ( $11.2 (E_{\text{max}}=16) < E^* < 12.4 (E_{\text{max}}=20)$  MeV). The simulations performed using the calculated GEF and Talys1.95 codes describe and predict the structure of mass distributions for a fissionable  $^{232}\text{Th}^*$  nucleus at an average excitation energy of  $\sim 11.3$  MeV.

## Acknowledgements

The authors would like to express their gratitude to the microtron group (I.I. Hainish, H.F. Pitchenko, O.M. Turkhovskiy) for the smooth operation of the accelerator and I.M. Kushtan for the technical support of experimental research.

## References

- [1] Mukhopadhyay T, Basu DN. Photonuclear reactions of actinides in the giant dipole resonance region. *Eur. Phys. J. A.* 2010;(45):121-24. <https://doi.org/10.1140/epja/i2010-10993-y>.
- [2] Schmidt K-H, Jurado B. Review on the progress in nuclear fission – experimental methods and theoretical descriptions. *Rep. Prog. Phys.* 2018;(81):article number 106301. <https://doi.org/10.1088/1361-6633/aacfa7>.
- [3] Experimental nuclear reaction data (EXFOR). Database Version of 2021-07-21. [Internet]. [updated 2021 July 21; cited 2021 Nov 5]. Available from: <https://www-nds.iaea.org/exfor/>.
- [4] Naik H, Kim GN, Suryanarayana SV, Kim KS, Lee MW, Sanjeev G, et al. Studies on neutron, photon (bremsstrahlung) and proton induced fission of actinides and pre-actinides. *J. Nucl. Phys. Mat. Sci. Rad. A.* 2015;(3):55-73. <https://doi.org/10.15415/jnp.2015.31008>.
- [5] Schmidt K-H, Steinhauser S, Bockstiegel C, Grewe A, Heinz A, Junghans AR, et al. Relativistic radioactive beams: A new access to nuclear-fission studies. *Nucl. Phys. A.* 2000;(665):221-67. [https://doi.org/10.1016/S0375-9474\(99\)00384-X](https://doi.org/10.1016/S0375-9474(99)00384-X).
- [6] Dubey R, Sugathan P, Jhingan A, Kaur G, Muku I, Mohanto G, et al. Interplay of fission modes in mass distribution of light actinide nuclei  $^{225,227}\text{Pa}$ . *Phys. Lett. B.* 2016;(752):338-43. <https://doi.org/10.1016/j.physletb.2015.11.060>.
- [7] Chatillon A, Taïeb J, Alvarez-Pol H, Audouin L, et al. Experimental study of nuclear fission along the thorium isotopic chain: From asymmetric to symmetric fission. *Phys. Rev. C.* 2019;(99):article number 054628. <https://doi.org/10.1103/PhysRevC.99.054628>.
- [8] Mathieu L, Heuer D, Merle-Lucotte E, Brissot R, Le Brun C, Liatard E, et al. Possible Configurations for the thorium molten salt reactor and advantages of the fast nonmoderated version. *Nucl. Sci. Eng.* 2009;(161):78-89. <https://doi.org/10.13182/NSE07-49>.
- [9] Sajo-Bohus L, Greaves ED, Davila J, Barros H, Pino F, Barrera MT, et al. Th and U fuel photofission study by NTD for AD-MSR subcritical assembly. *AIP Conf. Proc.* 2015;(1671):article number 020009. <https://doi.org/10.1063/1.4927186>.
- [10] Grdeň M. Non-classical applications of chemical analysis based on nuclear activation. *J Radioanal. Nucl. Chem.* 2020;(323):677-714. <https://doi.org/10.1007/s10967-019-06977-w>.
- [11] Naik H, Kim GN, Schwengner R, Kim K, John R, Massarczyk R, et al. Fission product yield distribution in the 12, 14, and 16 MeV bremsstrahlung-induced fission of  $^{232}\text{Th}$ . *Eur. Phys. J. A.* 2015;(51):article number 150. <https://doi.org/10.1140/epja/i2015-15150-8>.
- [12] Paşca H, Andreev AV, Adamian GG, Antonenko NV. Suggestion for examination of a role of multi-chance fission. *Eur. Phys. J. A.* 2018;(54):article number 104. <https://doi.org/10.1140/epja/i2018-12545-y>.
- [13] Tanaka S, Aritomo Y, Miyamoto Y, Hirose K, Nishio K. Effects of multichance fission on isotope dependence of fission fragment mass distributions at high energies. *Phys. Rev. C.* 2019;(100):article number 064605. <https://doi.org/10.1103/PhysRevC.100.064605>.
- [14] Tanaka S, Hirose K, Nishio K, Aritomo Y. Role of multichance fission in highly excited heavy nuclei. *JPS Conf. Proc.* 2020;(32):article number 010004. <https://doi.org/10.7566/JPSCP.32.010004>.
- [15] Schmidt K-H, Jurado B, Amouroux C, Schmitt C. General description of fission observables: GEF model code. *Nucl. Data Sheets.* 2016;(131):107-221. <https://doi.org/10.1016/j.nds.2015.12.009>.
- [16] GEF 2020/1.1 (A general description of fission observables) [Internet]. [updated 2020 December 15; cited 2021 Nov 6]. Available from: <http://www.khschmidts-nuclear-web.eu/GEF-2020-1-1.html>.
- [17] Raškinyte I, Dupont E, Morillon B, Ridikas D. Photonuclear data evaluation of actinides [Internet]. Varenna: Università degli Studi di Milano; 2006 [updated 2020 June 22; cited 2021 Nov 18]. Available from: [http://www0.mi.infn.it/~gadioli/Varenna2006/Proceedings/Dupont\\_E.pdf](http://www0.mi.infn.it/~gadioli/Varenna2006/Proceedings/Dupont_E.pdf).
- [18] Dupont E, Raškinyte I, Koning AJ, Ridikas D. Photonuclear data evaluations of actinides up to 130 MeV. International Conference on Nuclear Data for Science and Technology 2007. 2007;(ND 2007):article number 181. <https://doi.org/10.1051/ndata:07497>.
- [19] Talys 1.95 (release date: December 28, 2019) [Internet]. [updated 2020 April 20; cited 2021 Nov 6]. Available from: [https://tendl.web.psi.ch/tendl\\_2019/talys.html](https://tendl.web.psi.ch/tendl_2019/talys.html).
- [20] Piessens H, Jacobs E, De Frenne D, De Clercq A, Verboven M, De Smeet G. Photon induced fission of  $^{232}\text{Th}$  with 12 and 20 MeV bremsstrahlung. In: Seeliger D, Seidel K, Maerten H, editors. Proceeding of the XV<sup>th</sup> International Symposium on Nuclear Physics – Nuclear Fission. 1985; Gaussig. p. 92-95. [https://inis.iaea.org/search/search.aspx?orig\\_q=RN:19057645](https://inis.iaea.org/search/search.aspx?orig_q=RN:19057645).
- [21] Lendel AI, Maslyuk VT, Parlag OO, Sikora DI. Asymmetric modes of photo fission fragmentes mass distribution of the Th<sup>-232</sup>. *Scientific Herald of Uzhhorod University. Series "Physics"*. 1998;(3):24-6.

- [22] Byalko AA, Hudkov AN, Zhivun VM, Zvonarev AV, Kovalenko VV, Koldobskiy AV, et al. Experimental methods of nuclear physics. Vol. 3. Moscow: Atomizdat; 1978. Yields of  $^{235}\text{U}$  and  $^{239}\text{Pu}$  fission products by neutrons from the BR-1 fast reactor; 82-95.
- [23] Thierens H, De Frenne D, Jacobs E, De Clercq A, D'hondt P, Deruytter AJ. Study of the catcher foil technique with the aid of  $^{252}\text{Cf}$  (s. f.) and  $^{235}\text{U}$  (nth, f). *Nucl. Instr. Meth.* 1976;(134):299-308. [https://doi.org/10.1016/0029-554X\(76\)90285-8](https://doi.org/10.1016/0029-554X(76)90285-8).
- [24] GEANT4 10.7 (4 December 2020) [Internet]. [updated 2021 June 11; cited 2021 Nov 7]. Available from: <https://geant4.web.cern.ch/support/download>.
- [25] Evaluated nuclear data file (ENDF). Database version of 2021-03-19 [Internet]. [updated 2019 September 25; cited 2021 Nov 5]. Available from: <https://clck.ru/Wcz39>.
- [26] Parlag OO, Maslyuk VT, Dovbnaya AM, Pylypchynets IV, Holoveyi VM, Lendel OI, inventors; Institute of Electron Physics, National Academy of Sciences of Ukraine, patent holder. Method of manufacturing multinuclide gamma radiation source for calibration of semiconductor detectors by absolute efficiency. Patent of Ukraine No. 130235. 2018 Nov. 26.
- [27] Strilchuk MV. User manual for Winspectrum. Kyiv: Institute for Nuclear Research; unpublished. 120 p.
- [28] Decay Radiation data base version of 2/27/2021 [Internet]. [updated 2021 February 27; cited 2021 Nov 6]. Available from: [https://www.nndc.bnl.gov/nudat2/indx\\_dec.jsp](https://www.nndc.bnl.gov/nudat2/indx_dec.jsp).
- [29] Wahl AC. Nuclear-charge distribution and delayed-neutron yields for thermal-neutron-induced fission of  $^{235}\text{U}$ ,  $^{233}\text{U}$ , and  $^{239}\text{Pu}$  and for spontaneous fission of  $^{252}\text{Cf}$ . *ADNDAT*. 1988;38(1):1-156. [https://doi.org/10.1016/0092-640X\(88\)90016-2](https://doi.org/10.1016/0092-640X(88)90016-2).
- [30] Lengyel AI, Parlag OO, Maslyuk VT, Romanyuk MI, Gritzay OO. Calculations of average numbers of prompt neutrons for actinide photofission. *Journal of Nuclear and Particle Physics*. 2016;6(2):43-6.

## Структура масових розподілів виходів продуктів фотоподілу $^{232}\text{Th}$ гальмівним випромінюванням з енергією 17.5 MeV

Олег Олександрович Парлаг, Володимир Трохимович Маслюк, Євген Володимирович Олейніков, Ігор Васильович Пилипчинець, Олександр Іванович Лендел

Інститут електронної фізики НАН України  
88017, вул. Університетська, 21, м. Ужгород, Україна

### Анотація

**Актуальність.** Одним з найбільш перспективних напрямів вивчення процесу поділу є вивчення його особливостей під дією фотонного випромінювання, оскільки взаємодія гамма-квантів з ядром є повністю електромагнітною з добре відомими характеристиками. Особливий інтерес з точки зору експериментальних і теоретичних досліджень представляє інформація про виходи продуктів фотоподілу ядра  $^{232}\text{Th}$ , яке знаходиться на межі між до-актинідами та легкими актинідами.

**Мета.** Метою роботи є експериментальне дослідження структури масового розподілу виходів продуктів фотоподілу  $^{232}\text{Th}$  за енергії 17.5 MeV (енергії, близької до порогу першого шансу поділу, де відсутні експериментальні дані).

**Методи.** Стимуляція реакції фотоподілу  $^{232}\text{Th}$  проводилася на електронному прискорювачі Інституту електронної фізики України – мікротроні М-30. Спектр гальмівного випромінювання моделювався для випадку взаємодії електронів ( $E = 17.5$  MeV) з танталовим конвертером (1 мм) за допомогою коду GEANT4 10.7. Виходи продуктів фотоподілу  $^{232}\text{Th}$  вимірювалися гамма-спектрометричним методом. Моделювання виходів продуктів фотоподілу  $^{232}\text{Th}$  виконано за допомогою кодів GEF 2020 / 1.1 і Talys 1.95.

**Результати.** Значення 23 кумулятивних виходів продуктів ( $^{85\text{m}}\text{Kr}$ ,  $^{88}\text{Kr}$ ,  $^{88}\text{Rb}$ ,  $^{89}\text{Rb}$ ,  $^{91}\text{Sr}$ ,  $^{92}\text{Sr}$ ,  $^{94}\text{Y}$ ,  $^{95}\text{Zr}$ ,  $^{97}\text{Nb}$ ,  $^{99}\text{Mo}$ ,  $^{101}\text{Tc}$ ,  $^{131}\text{I}$ ,  $^{132}\text{Te}$ ,  $^{133}\text{I}$ ,  $^{134}\text{Te}$ ,  $^{135}\text{I}$ ,  $^{138}\text{Cs}$ ,  $^{139}\text{Ba}$ ,  $^{140}\text{Ba}$ ,  $^{141}\text{Ce}$ ,  $^{142}\text{La}$ ,  $^{143}\text{Ce}$ ,  $^{146}\text{Ce}$ ), що належать 22 ізобарним масовим ланцюжкам (легкі: 85; 88; 89; 91; 92; 94; 95; 97; 99; 101, важкі: 131; 132; 133; 134; 135; 138; 139; 140; 141; 142; 143; 146 уламки) фотоподілу  $^{232}\text{Th}$  були виміряні при максимальній енергії гальмівного випромінювання 17.5 MeV (середня енергія збудження  $\sim 11.3$  MeV). Отриманий масовий розподіл важких фрагментів вказує на наявність підвищених виходів продуктів, локалізованих в області мас 133-134, 138-139 і 143-144, що пов'язано з впливом такої ядерної структури, як близькість замкнених ядерних оболонок і парно-непарний ефект.

**Висновки.** Результати вимірювань вказують на наявність тонкої структури в отриманому масовому розподілі виходів продуктів фотоподілу  $^{232}\text{Th}$ , що проявляється у збільшених виходах продуктів, локалізованих в області мас 133-134, 138-139 і 143-144. Отримані теоретичні значення виходів, розраховані з використанням кодів GEF 2020 / 1.1 і Talys 1.95, в загальних рисах описують і прогнозують тонку структуру масового розподілу виходів продуктів фотоподілу  $^{232}\text{Th}$

**Ключові слова:** гальмівне випромінювання, мікротрон,  $^{232}\text{Th}$ , гамма-спектрометрія, перший шанс поділу